Mass Profiles and Shapes of Cosmological Structures
G. Mamon, F. Combes, C. Deffayet, B. Fort (eds)
EAS Publications Series, Vol. ?, 2005

OBSERVATIONS OF INFALL AND CAUSTICS

R. Brent Tully[1]

Abstract. Identification of first and second turnaround radii in groups of galaxies provide interesting scaling relations and may constrain cosmological parameters.

1 Introduction

Collapse timescales, t_c, depend on the density, ρ, of a bound structure which in turn depends on the mass, M, enclosed within a radius, r: $t_c \sim \rho^{-1/2} \sim (r^3/M)^{1/2}$. For two structures at the same phase of collapse today:

$$r_1 = r_2(M_1/M_2)^{1/3}. \tag{1.1}$$

Suppose we are comparing structures within the radius of second turnaround, r_{2t}, the maximum radius that a collisionless object reaches upon falling once through the center of the group potential. The dynamical stages of the two comparison groups are similar so $M \sim \sigma_V^2 r_{2t}$ where σ_V is the velocity dispersion within the quasi-virialized region bounded by r_{2t}. If we consider $t =$ today, then $(\sigma_V^2 r_{2t}/r_{2t}^3)^{1/2} =$ constant and:

$$\sigma_V \sim r_{2t}. \tag{1.2}$$

2 Observations of the caustic of second turnaround

Models of spherical infall of cold, collisionless particles (Bertschinger 1985, ApJS, 58, 39) suggest that the radius of second turnaround r_{2t} will be marked by a density drop and a transition from a large velocity dispersion interior to r_{2t} to cold infall exterior to r_{2t}. Projection effects in the real world might make the cold infall difficult to distinguish, but that is a matter to be explored below. The theoretical models also predict density cusps at the 2nd and all interior turnarounds but it can be presumed that these features would be wiped out in the real world with asphericity, finite peculiar motions, and collisions.

[1] Institute for Astronomy, University of Hawaii, Honolulu, Hawaii, 96822 USA

DOI: (will be inserted later)

It is not surprising that the caustic of 2nd turnaround has received little observational attention because the anticipated density transition is subtle and velocity effects are obscured by projection. Fortunately, in a recent study (Mahdavi et al. 2005, AJ, astro-ph/0506737) a particularly clean case came to light. The modest but dense group of early-type galaxies around NGC 5846 lies within the Local Supercluster at 26 Mpc in relative isolation. The group is a knot within a filament that lies close to the plane of the sky and the space to the foreground and back are voids. The group has a huge dwarf population with 325 candidate members and, overall, velocities are available for 85 affirmed members. The NGC 5846 group has a velocity dispersion of 322 km s^{-1} and a mass of $8 \times 10^{13} M_{\odot}$.

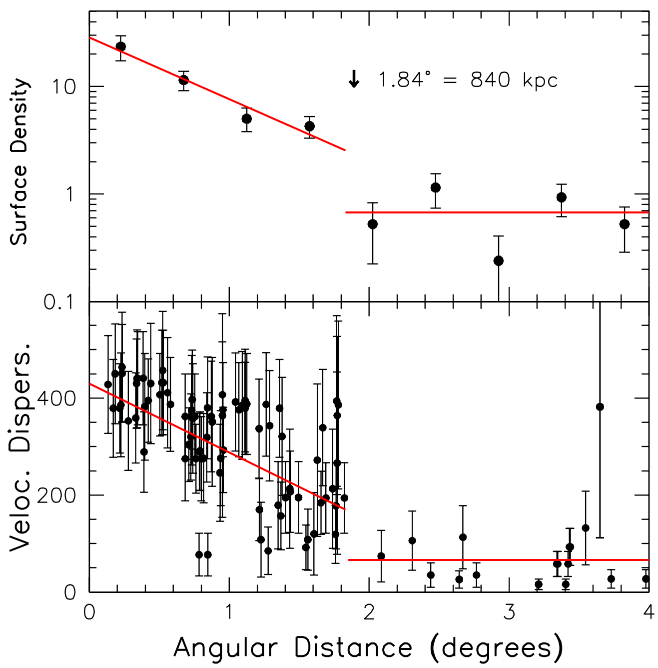

Fig. 1. Radial gradients. *Top:* Surface density dependence on radius for galaxies with observed velocities and $R < 17.2$. The surface density drops smoothly with radius out to $\sim 1.8^{\circ}$ then drops abruptly to a roughly constant value. *Bottom:* Velocity dispersion as a function of radius. Each data point represents the velocity dispersion of all galaxies within 0.5 Mpc of individual galaxies considered one at a time; thus, the data points are not independent. The sloping line within 1.8° is fit to velocity dispersions averaged over the 4 annular bins of the top panel. The flat line, showing the mean velocity dispersion outside 1.8°, lies at 66 km s^{-1}.

Figure 1 summarizes the pertinent observations. Sloan Digital Sky Survey velocities are available for all galaxies in the region with $R < 17.2$ which provides a complete magnitude limited sample uncontaminated by background. The top

panel of Fig. 1 shows the run of surface densities and the bottom panel shows the run of velocity dispersions. The latter, to be precise, is the velocity dispersion in small windows centered at each galaxy in the sample. The point is to show the *very small dispersions* in local regions at large radii, the signature of cold infall. If dispersions were averaged over annuli then the cold flow at large radii would be camouflaged by projection differences between widely separated galaxies. The anticipated transition at r_{2t} is seen at $1.84^\circ = 840$ kpc.

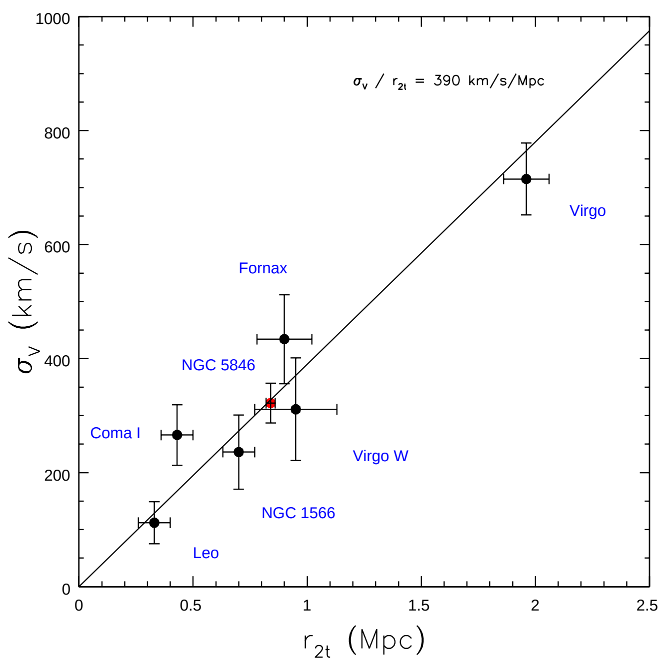

Fig. 2. Correlation between velocity dispersion and inferred radius of 2nd turnaround for E/S0 knots in Local Supercluster.

The locations of 2nd turnaround are less certainly defined for other nearby knots of E/S0 galaxies but rough estimates are available. Those estimates give rise to the correlation seen in Figure 2. The straight line describes the relation anticipated by Eq. 1.2:

$$\sigma_V / r_{2t} = 390 \text{ km s}^{-1} \text{ Mpc}^{-1} \qquad (2.1)$$

3 The ratio of first to second turnaround radii

The ratio of the radii of first and second turnaround, r_{1t}/r_{2t}, depends on cosmology. Mamon (private communication) finds the related ratio r_{1t}/r_{vir} ranges between 3.1 and 3.7 for $0 < \Omega_m < 1$ in a flat Universe. The best shot at defining

r_{1t} with present data lies with the Local Group because in this unique circumstance we see almost the entire vector of radial infall motion. The radii r_{2t} around the Milky Way (MW) and M31 can be inferred from Eq. 2.1 or from the variant that follows from Eq. 1.1. Given mass estimates for these galactic systems of $1 \times 10^{12}\ M_{\odot}$ (Wilkinson & Evans 1999, MNRAS, 310, 645; Evans et al. 2000, ApJ, 540, L9) then $r_{2t} \sim 200$ kpc. It is seen in Figure 3 that 200 kpc is roughly the domain of the gas poor and high velocity dispersion galaxies around M31 and MW. Beyond this radius, galaxies are mostly gas rich and have velocities indicative of infall. The transition to blueshifts, marking the surface of first turnaround, occurs at a radius $r_{1t} \sim 900$ kpc. In principle, the ratio r_{1t}/r_{2t} provides a constraint on Ω_m. The present observed parameters are soft because of the small number of Local Group galaxies and the dumbbell shape of the potential. In any event, it would be nice to see what simulations anticipate in similar circumstances.

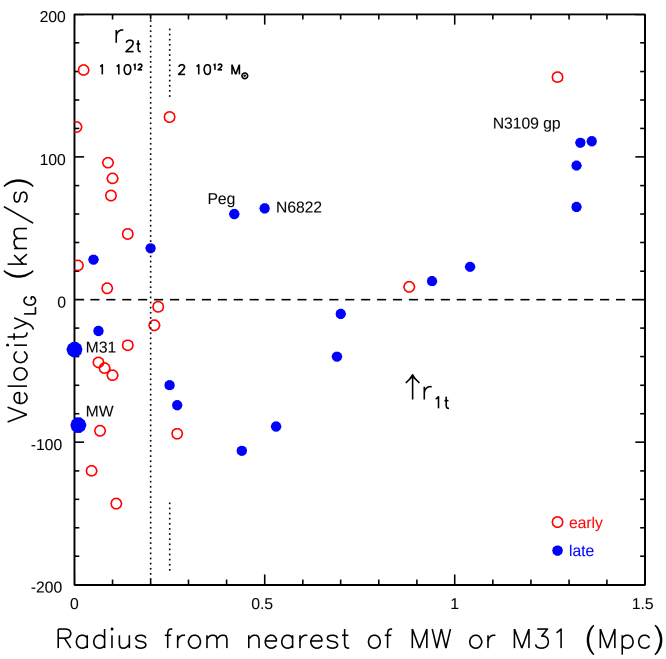

Fig. 3. Discrete quasi-virialized and infall regions within the Local Group. Velocities with respect to the centroid of the Local Group are plotted against the distance of a galaxy from the *nearer* of M31 or the Milky Way. Locations of 2nd turnaround for M31 and M31 are scaled using Eq. 1.1 from the relation for E/S0 knots shown in Fig. 2. The approximate position of the 1st turnaround for the combined M31+MW system is also indicated.